Journal of Neurochemistry, 2005, **95**, 553–562 doi:10.1111/j.1471-4159.2005.03411.x

Effects of CAG repeat length, HTT protein length and protein context on cerebral metabolism measured using magnetic resonance spectroscopy in transgenic mouse models of Huntington's disease

Bruce G. Jenkins,* Ole A. Andreassen,† Alpaslan Dedeoglu,‡ Blair Leavitt,§ Michael Hayden,§ David Borchelt,¶ Christopher A. Ross,¶ Robert J. Ferrante‡ and M. Flint Beal**

**MGH-NMR Center, Department of Radiology, Massachusetts General Hospital and Harvard Medical School, Charlestown, Massachusetts, USA*

†Neurochemistry Laboratory, Neurology Service, Massachusetts General Hospital and Harvard Medical School, Boston, Massachusetts, USA

‡Geriatric Research Education and Clinical Center, Bedford VA Medical Center, Bedford, Massachusetts, USA and Department of Neurology, Pathology, and Psychiatry, Boston University School of Medicine, Boston, Massachusetts, USA

§Centre for Molecular Medicine and Therapeutics, University of British Columbia, Vancouver, Canada

¶Departments of Neurology, Psychiatry and Neuroscience, Johns Hopkins University, Baltimore, Maryland, USA

***Department of Neurology and Neuroscience, Weill Medical College of Cornell University, New York Presbyterian Hospital, New York, USA*

Abstract

Huntington's disease is a neurodegenerative illness caused by expansion of CAG repeats at the N-terminal end of the protein huntingtin. We examined longitudinal changes in brain metabolite levels using *in vivo* magnetic resonance spectroscopy in five different mouse models. There was a large (>50%) exponential decrease in *N*-acetyl aspartate (NAA) with time in both striatum and cortex in mice with 150 CAG repeats (R6/2 strain). There was a linear decrease restricted to striatum in N171-82Q mice with 82 CAG repeats. Both the exponential and linear decreases of NAA were paralleled in time by decreases in neuronal area measured histologically. Yeast artificial chromosome transgenic mice with 72 CAG repeats, but low expression levels, had less striatal NAA loss than the N171–82Q mice (15% vs. 43%). We evaluated the effect of gene context in mice with an approximate 146 CAG repeat on the hypoxanthine phosphoribosyltransferase gene (HPRT). HPRT mice developed an obese phenotype in contrast to weight loss in the R6/2 and N171–82Q mice. These mice showed a small striatal NAA loss (21%), and a possible increase in brain lipids detectable by magnetic resonance (MR) spectroscopy and decreased brain water T1. Our results indicate profound metabolic defects that are strongly affected by CAG repeat length, as well as gene expression levels and protein context.

Keywords: Huntington's disease, magnetic resonance spectroscopy, *N*-acetyl aspartate, neuronal area, transgenic mice.

J. Neurochem. (2005) **95,** 553–562.

Huntington's disease (HD) is an autosomal, dominant, inherited, neurodegenerative disorder characterized by a progressive development of motor, cognitive and psychiatric

Received February 16, 2005; revised manuscript received June 10, 2005; accepted June 14, 2005.

Address correspondence and reprint requests to Bruce G. Jenkins, MGH-NMR Center, Department of Radiology, Massachusetts General Hospital and Harvard Medical School, Charlestown, MA 02129, USA. E-mail: bgj@nmr.mgh.harvard.edu

Abbreviations used: HD, Huntington's disease; HPRT, hypoxanthine phosphoribosyltransferase; MRS, magnetic resonance spectroscopy; NAA, *N*-acetyl aspartate; SNR, signal-to-noise ratio; YAC, yeast artificial chromosome.

symptoms, with an initial neurodegeneration in the basal ganglia that later can affect multiple brain regions. The genetic defect that causes the illness was identified as an expanded CAG/polyglutamine repeat in a 350 kDa protein, (Untington's Disease Collaborative Research Group 1993). Recent evidence suggests that the CAG repeat confers a gain of function that may be related to interference with gene transcription (Lin *et al*. 2000; Luthi-Carter *et al*. 2000; Nucifora *et al*. 2001). Mutant huntingtin appears to interfere with vesicular transport of neuroprotective molecules such as BDNF (Gauthier *et al*. 2004), but the ultimate pathogenic mechanism of the disease is not yet known, and no effective treatment is available.

Normal individuals possess a repeat length of 6–35 glutamines, whereas HD is present when alleles of more than approximately 36 repeats are inherited. The onset of HD is usually in mid-life with a mean survival of 15–20 years after onset, and the age of onset and the severity of the disease are correlated with the length of the CAG expansion (Andrew *et al*. 1993; Snell *et al*. 1993). A major advance in HD research was the development of transgenic mouse models. A number of strains has been created with different numbers of repeats as well as different fractions of the gene. One of the first strains created was the R6/2 mice. These mice express an N-termimal fragment (exon-1 only) of the human HD gene with 150 CAG repeats and develop a progressive neurological disorder with features similar to juvenile onset HD (Mangiarini *et al*. 1996). At 6 weeks-of-age, the R6/2 mice develop loss of body and brain weight; at 9–11 weeks, they develop an irregular gait, abrupt shuttering stereotypic movements, resting tremor and epileptic seizures, and they die at around 100 days-of-age (Mangiarini *et al*. 1996). The brains show striatal neuronal atrophy without much neuronal cell loss and intranuclear inclusions that are immunopositive for huntingtin and ubiquitin (Davies *et al*. 1997; Ferrante *et al*. 2000). Another strain, referred to as N171-82Q mice, express a cDNA encoding a 171 amino acid N-terminal fragment of huntingtin containing 82 CAG repeats (Schilling *et al*. 1999). These mice show similar symptoms to the R6/2 mice, but have a more delayed disease onset and longer survival, with the phenotype beginning at about 90 days-of-age and average death at around 135 days-of-age (Schilling *et al*. 1999; Andreassen *et al*. 2001b). These mice also show selective striatal pathology, unlike the R6/2 mice where the striatum and cortex are equally affected. Hayden and co-workers produced yeast artificial chromosome (YAC) transgenic mice expressing mutant huntingtin with 72 CAG repeats (YAC72) (Hodgson *et al*. 1999). Two strains of these mice were developed, one with a relatively normal expression level of htt (line 2498) and the other with a low expression level of htt (line 2511). The 2498 line has a similar disease phenotype as the R6/2 and N171-82Q mouse models above but an even later onset, with electrophysiological abnormalities from 6 months of age and striatal neurodegeneration appearing at 12 months of age (Hodgson *et al*. 1999). The 2511 strain has milder symptoms still and has a very mild phenotype. The use of these mice thus allows for comparison of the effects of expression levels as well as CAG repeat length. In addition, in order to determine the effects of gene context, we studied a model in which an expanded CAG repeat is introduced into the mouse hypoxanthine phosphoribosyltransferase gene (Hprt) (Ordway *et al*. 1997). These mice develop motor abnormalities and nuclear inclusions similar to the other mice, but also have many different phenotypic characteristics, such as weight gain compared with weight loss for most of the other HD models.

Magnetic resonance spectroscopy (MRS) has shown a loss of *N*-acetyl aspartate (NAA), a marker of neuronal health and viability, in the striatum in HD patients (Jenkins *et al*. 1993, 1998; Hoang *et al*. 1998; Sanchez-Pernaute *et al*. 1999) that is also seen using *in vitro* methods (Dunlop *et al*. 1992). MRS has also shown loss of NAA in transgenic mouse models of HD (Jenkins *et al*. 2000; van Dellen *et al*. 2000) which correlates with *in vitro* HPLC or NMR measurements (Jenkins *et al*. 2000). Transgenic HD mice of the R6/2 strain show a rapid loss of NAA in the absence of neuronal cell loss in the striatum, and an increase in glucose and glutamine levels as well as large increases in taurine and scyllo-inositol (Jenkins *et al*. 2000). Increases in extracellular glutamine and taurine, and impaired uptake of extracellular glutamate measured using microdialysis, have also recently been found in the R6/2 mice (Behrens *et al*. 2002). In the present study, we examined the longitudinal changes in brain metabolite levels using *in vivo* MRS in the R6/2 and N171-82Q transgenic HD mouse models. Furthermore, we made comparisons with the YAC72 and HPRT mice at single time points.

Methods

Animals

Male transgenic HD mice of the R6/2 strain were obtained from Jackson Laboratories (Bar Harbor, ME, USA). The male R6/2 mice were bred with females from their background strain (B6CBAFI/J) for six generations. The offspring were genotyped by a PCR radioassay method on DNA obtained from tail tissue (Wheeler *et al*. 1999); this ensured that the number of CAG repeats was the same in all the offspring. Littermate transgene negative animals were used as controls. Male transgenic HD mice of the N171-82Q line (hybrid background strain C3H/HEJ × C57BL/6JF1), which have 82 CAG repeats, were obtained from Drs Borchelt and Ross, and bred with female B6C3F1 mice (Jackson Laboratories) for five generations; male N171-18Q mice with 18 CAG repeats and no underlying clinical phenotype were bred with female B6C3F1 mice for one generation. The offspring were genotyped with a PCR assay on tail DNA (Schilling *et al*. 1999). Transgenic mice of the YAC72 strain (background strain FVB/N) with the full-length mutant human htt

were obtained from the laboratory of Drs Blair Leavitt and Michael Hayden, where they had been genotyped with PCR assay from tail DNA (Hodgson *et al*. 1999). Littermate controls who were transgene negative were used for these mice. It should be noted that the YAC72 mice we studied were the 2511 line and not the 2498 line reported in Hodgson *et al*. (1999). The latter expresses the mutant human htt at higher levels than the 2511 line, and the 2511 line has a much milder phenotype. Transgenic mice (from line JO1/C57BL/6J) with an approximate 146 length CAG repeat at the N-terminal end of the full-length hypoxanthine phosphoribosyltransferase (HPRT) gene were obtained from Dr Peter Detloff (Ordway *et al*. 1997). The HPRT mice had an average age of 191 ± 16.2 days.

The mice were housed under standard conditions with free access to water and food. All animal experiments were carried out in accordance with the NIH Guide for the Care and Use of Laboratory Animals and were approved by the local animal care committee. Unless otherwise noted, all errors reported are standard deviations.

Neuronal area measurements

Striatal neuronal areas were analyzed by microscopic videocapture (Optimas; Bioscan Incorporated, Edmonds, WA, USA) using methodology described in detail elsewhere (Ferrante *et al*. 2000; Andreassen *et al*. 2001b). Neurons automatically identified by the system were manually verified to be neurons.

Magnetic resonance spectroscopy (MRS) and imaging

In vivo MRS was collected with a Point Resolved Spectroscopy Sequence (PRESS) sequence using a GE Omega 4.7T imager (GE, Fremont, CA, USA) and a home made 20 mm sinusoidal bird cage coil using a TR of 2000 ms and two TE values (136 and 272 ms), as described in detail earlier (Jenkins *et al*. 2000; Dedeoglu *et al*. 2004). Voxels were placed symmetrically about both basal ganglia (average size of $6 \times 3.5 \times 3$ mm, ≈ 63 ml) or over the motor cortex ($6 \times 2 \times 3$ mm, ≈ 36 ml). Based upon segmentation of T2-weighted images, the cortical voxels were found to consist of approximately 60% sensory/motor cortex, 15% cingulate, 15% parietal, 5% corpus callosum and 5% non-brain. Approximately half-way through the study, a new pre-amp and TR switch were added to the machine and this resulted in a gain in signal-to-noise ratio (SNR) of approximately 70%. These spectra were pooled; since the results are reported as ratios to creatine, this will have minimal effect. Spectra in which the SNR of the creatine peak was less than 8 were not analyzed. Mice were imaged under halothane/N_2O/O_2 anesthesia (1–1.5% halothane) and maintained at 38°C using a circulating water blanket. Spectra were analyzed by fitting the spectra to mixed Gaussian-Lorenzian lineshapes and then integrating. Spectra were integrated and normalized to the creatine/phosphocreatine peak, which our prior HPLC measurements showed to be identical in HD and control animals (Jenkins *et al*. 2000). Brain size was measured in a subset of the R6/2 ($n = 8$) and wild-type mice ($n = 6$) using eight consecutive 1 mm slices from T2-weighted MRI images (TR/TE 3200/65 ms; FOV 40 mm; 256 × 128 zero-filled to 256 × 256). The total volume of the eight slices was summed using automated software that counts total pixels within the brain outline determined from intensity contours. Measurements of the longitudinal relaxation time T1 were made in wild-type, R6/2 and HPRT mice using sequential spin-echo saturation-recovery experiments with 12–14 TR values between 80 ms and 5 s. Data were fitted to two parameters [T1 and fully relaxed signal at infinite recovery S(inf)] in a single exponential curve as S(TR) = S(inf)*(1-exp(-TR/T1)).

Comparisons of metabolite levels were run using one-way ANOVA. Curve fit comparisons were compared using both an *F*-test as well as an *R*-factor ratio test (Hamilton 1965).

Results

Shown in Fig. 1 are T2-weighted images of a mouse with typical voxels selected (also shown are images of the voxels using the PRESS sequence). These mice have increased ventricular size compared with the wild-type mice. They also show a decrease in brain size. We measured brain size using the T2-weighted MRI images in six wild-type and eight R6/2 mice at 10 weeks-of-age. Brain size was decreased in the R6/2 mice compared with the wild-type by 12.2% ($p < 0.005$). This compares quite well with a decrease in brain weight in fixed specimens of R6/2 mice (compared with wild-type), at approximately the same age, of 11.8% that we measured previously (Ferrante *et al*. 2000).

Shown in Fig. 2 are representative striatal spectra for the N171-82Q and YAC-72 mice. Although both strains have similar CAG repeat numbers, there is a large decrease in NAA as well as an increase in taurine in the N171-82Q mice, whereas the YAC-72 mice show only a small decrease in NAA. The NAA levels noted in the YAC-72 mice are similar to those seen in the N171-18Q mice. In both of these latter two strains, however, NAA values are lower than in the wild-type controls (see Table 1). In Fig. 3, representative spectra are shown for the R6/2 mice and wild-type mice. There is a large decrease in NAA as well as an increase in taurine and glutamine in the R6/2 mice, as we reported earlier (Jenkins *et al*. 2000); there is also a bigger lactate peak [the inverted peak at 1.33 ppm, similar to that which we have found in humans (Jenkins *et al*. 1998)]. The average lactate/creatine

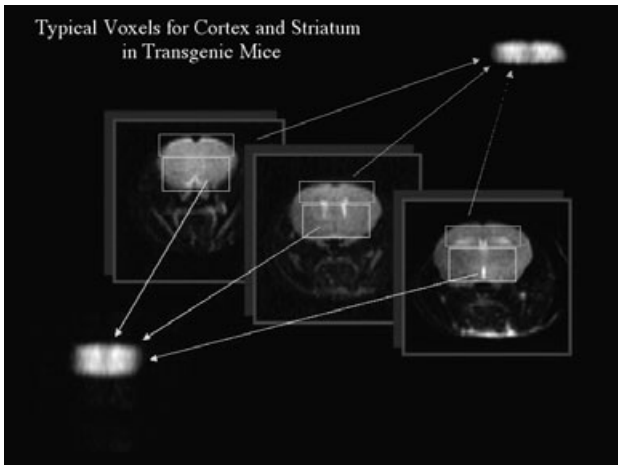

Fig. 1 T2-weighted images and typical MRS voxels in an R6/2 mouse.

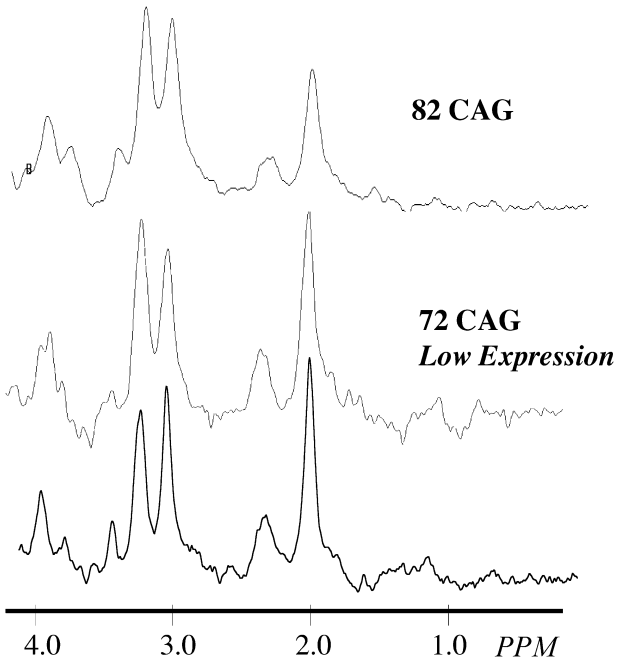

Fig. 2 Representative PRESS spectra (TR/TE 2000/136 ms) from the striatum in N171-82Q mice with 82 CAG repeats (top), YAC72 mice with 72 CAG repeats but low expression levels (middle) and a wild-type littermate YAC mouse (bottom).

level was 0.14 ± 0.06 in the R6/2 mice and was unobservable (and hence unquantifiable) in the wild-type mice.

We performed longitudinal analysis of metabolite levels using NMR spectroscopy *in vivo*. There was a large decrease in NAA in both the striatum and cortex in the R6/2 mice, but only in the striatum in the N171-82Q mice (see Fig. 4 and Table 1). Changes in the ^{1}H MRS spectra as a function of time in the striatum and cortex in a single N171-82Q mouse are shown in Fig. 4(a). It can be seen that the striatal spectra change dramatically as a function of age. The cortical spectrum at 134 days-of-age is not dramatically different from a wild-type spectrum at the same age. The decrease in NAA as a function of time in the striatum is shown for all the N171-82Q and N171-18Q repeat mice in Fig. 4(b). Note the steep linear decrease in NAA over time in the N171-82Q mouse ($p < 0.001$). Even the N171-18Q mice, which demonstrate no profound neurological phenotype, have striatal spectra that show a small linear decrease in NAA with time ($p = 0.086$). Also shown in Fig. 4(b) are data on neuronal area. It is clear that there is a linear decrease in neuronal area that parallels the decreases noted in NAA in the N171-82Q mice. The slopes, when normalized to the pre-symptomatic values, are similar. The neuronal areas as a function of time are reported in Table 2.

We previously reported an exponential decrease in NAA in the R6/2 mice (Jenkins *et al*. 2000). Shown in Fig. 5 are data from an expanded data set with 15 more mice than reported previously. We fit the data to the following function :

$$\mathrm{NAA(obs)} = \mathrm{NAA(d)} + [\mathrm{NAA(p)} - \mathrm{NAA(d)}] * \exp -[(\mathrm{age} - \mathrm{AO})/\mathrm{NAA(t)}]$$

where NAA(obs) is the observed NAA value, NAA(p) is the pre-symptomatic NAA value (taken to be the wild-type value), NAA(d) is the average value of NAA at the average age of death (about 14 weeks in these mice), NAA(t) is the time constant for NAA decay, and AO is the age at which the NAA starts to become abnormal (age of onset as determined by the NAA metric). We fitted the data shown in Fig. 5 to the full data set or the binned data at approximately weekly intervals. In the former case, the age of onset, AO, was determined to be 5.0 ± 0.4 weeks and in the latter case, it was 5.4 weeks. The data fit significantly better to a two-parameter exponential function compared with a linear function ($p < 0.001$ using either an *F*-test or an *R*-factor ratio test). Also shown in Fig. 5 are data we presented previously on neuronal area measured stereologically in the R6/2 mice (Ferrante *et al*. 2000). These results (albeit with only four time points) show an exponential-like decrease with time that parallels that of the NAA, suggesting a mechanism for the NAA loss. These exponential-like drops in NAA and neuronal area are to be contrasted with the linear decrease noted in the 82 CAG repeat mice shown in Fig. 4 above.

Taurine and choline increased linearly with time in the striatum in both the R6/2 and N171-82Q mice (not shown). The taurine increase was not significant in the cortex in any of the mice except the R6/2 strain. We showed previously that NAA did not change significantly in wild-type mice over time (Jenkins *et al*. 2000). The spectroscopic data are summarized for all four different strains of mice, as well as the wild-type mice, in Table 1. In order to facilitate comparisons, we averaged data for all time points, except for the R6/2 mice where the large numbers of animals allowed for comparisons at 11–12 weeks, which was closer in age to the wild-type mouse measurements.

We also measured spectra in the HPRT mice with approximately 146 CAG repeats. The median age of death in these mice is about 45 weeks-of-age (Ordway *et al*. 1997). These mice also show a dramatically increased body weight compared with wild-type mice, in contrast to the R6/2 mice which lose about 30% of their body weight by 13 weeks of age. Peak body weight in the HPRT mice was 48.4 ± 2.3 g versus 18.8 g in the R6/2 mice, 25.8 ± 1.1 g in the N171-82Q mice and 33.9 ± 4.6 g in the N171-18Q mice. The HPRT mice had an unusual accumulation of free lipid-like molecules in the striatum. Shown in Fig. 6 are spectra from the striatum at both 136 and 272 ms TE values. There are a number of peaks of various phase between 0 and 2 ppm. These resonances disappear at the longer echo time of 272 ms, due to their

Table 1 Changes in neurochemicals as a function of CAG repeat in transgenic HD mouse models

Mouse	NAA	Glx	Cho	Taurine
R6/2 Striatum ($n = 16$)	0.70 ± 0.1[a]	0.45 ± 0.21	1.21 ± 0.15[a]	0.34 ± 0.06[a]
R6/2 Cortex ($n = 8$)	0.68 ± 0.1[a]	0.44 ± 0.18	1.1 ± 0.08[a]	0.32 ± 0.09[a]
N171-82Q Striatum ($n = 21$)	0.82 ± 0.1[a,b]	0.38 ± 0.14	1.1 ± 0.17	0.31 ± 0.1[a,b]
N171-82Q Cortex ($n = 11$)	1.26 ± 0.14	0.26 ± 0.06	0.91 ± 0.14	0.17 ± 0.05
N171-18Q Striatum ($n = 14$)	1.13 ± 0.09 [a,b]	0.26 ± 0.11	1.0 ± 0.25	0.20 ± 0.04
N171-18Q Cortex ($n = 5$)	1.40 ± 0.31	0.26 ± 0.1	0.88 ± 0.06	0.16 ± 0.05
YAC 72 Striatum ($n = 5$)	1.21 ± 0.1[a,b]	0.44 ± 0.11	1.25 ± 0.2 [a,b]	0.32 ± 0.12
YAC 72 Cortex ($n = 5$)	1.46 ± 0.28	0.26 ± 0.13	0.86 ± 0.08	0.20 ± 0.09
YAC WT Striatum ($n = 6$)	1.39 ± 0.12	0.33 ± 0.11	1.01 ± 0.16	0.21 ± 0.07
YAC WT Cortex ($n = 5$)	1.45 ± 0.12	0.29 ± 0.06	0.86 ± 14	0.24 ± 0.03
R6/2 WT Striatum ($n = 9$)	1.43 ± 0.17	0.29 ± 0.09	0.82 ± 0.11	0.21 ± 0.07
R6/2 WT Cortex ($n = 7$)	1.50 ± 0.30	0.29 ± 0.11	0.82 ± 0.16	0.23 ± 0.04

[a]Significantly different from appropriate wild-type value. [b]Significantly different from cortex value in the same animals. WT, wild-type. These data are averages over all time points except for the CAG 150 data which is at 11-12 weeks. Intensities are expressed as relative to creatine. Means ± standard deviations are presented. Spectra were collected at echo times of 136 ms.

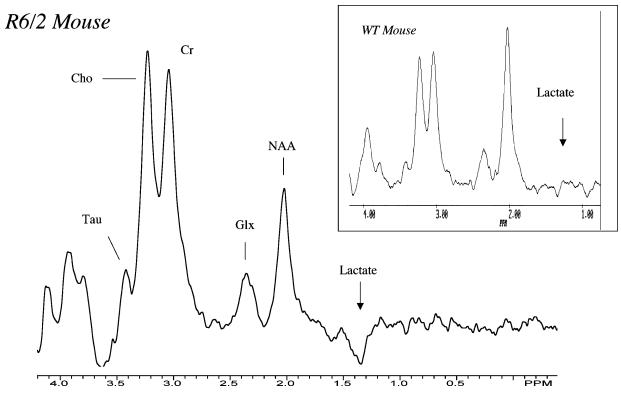

Fig. 3 Representative PRESS spectra (TR/TE 2000/136 ms) from the striatum in R6/2 mice with an inset showing a spectrum from wild-type mice. There is a large decrease in NAA, and increases in lactate (the inverted peak at 1.33 ppm), choline and taurine.

short T2s. We note that these spectra arise from striatum far from scalp lipids. They were not seen in any of the other mouse models using the same coil and pulse sequence and therefore, they are unlikely to represent scalp lipids. The increased brain lipids are also reflected in a decreased brain T1 value. Shown in Fig. 7 are T1 relaxation curves from the striatum in wild-type and HPRT mice. Also shown is a bar graph of T1 values in the striatum and cortex in wild-type, R6/2 and HPRT mice. The R6/2 mice show a small increase in T1 values compared with the wild-type, whereas the T1 is approximately 30% shorter in the HPRT mice. Due to the interference of the lipid-like resonances, we quantified the striatal data for the HPRT mice at 272 ms echo times. These data are shown in Table 3 along with values for the wild-type spectra at the same echo time.

Discussion

The results indicate a profound metabolic defect in these transgenic mice that is strongly affected by CAG repeat length. It is worthwhile summarizing some of the findings in these mice relevant to our data. Consistent with its long CAG expansion, the R6/2 model has the most severe phenotype and also shows the most profound changes in NMR spectra. These mice have a large loss of NAA in both the striatum and cortex. The NAA loss is highly non-linear with time, fitting well to an exponential function with an age of onset of about 5 weeks, and parallels in time the decreases in neuronal area. We previously showed that these mice have changes in a number of other brain metabolites, most notable being large increases in glutamine and small decreases in glutamate

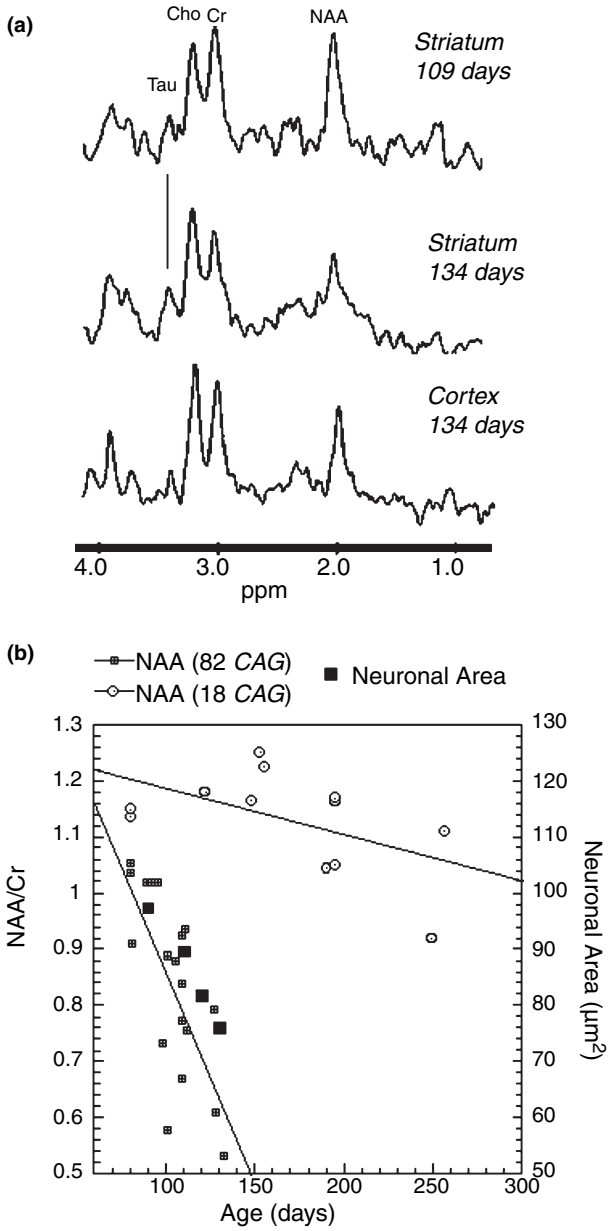

Fig. 4 (a) Spectra from the same N171-82Q mouse at various time points in striatum and cortex. Note the much larger NAA loss in striatum than in cortex. (b) Plot of loss in NAA over time in N171-82Q mice and N171-18Q (18 CAG repeats). There is a much steeper decline in NAA in the 82 CAG mice than in the 18 CAG mice. The loss in NAA correlates with the loss in neuronal areas measured histologically. Both NAA and neuronal area loss fit well to a linear function.

Table 2 Neuronal areas in N171-82Q and wild-type mice as a function of age

Age	Wild-type	N171-82Q
90 days	102.3 ± 7.9 μm²	97.4 ± 10.2 μm²
110 days	105.6 ± 8.2 μm²	89.7 ± 11.7 μm²
120 days	112.4 ± 6.4 μm²	81.8 ± 15.2 μm²
130 days	114.2 ± 10.1 μm²	76.1 ± 12.6 μm²

Ten animals were assayed per group. Numbers are means ± standard deviations.

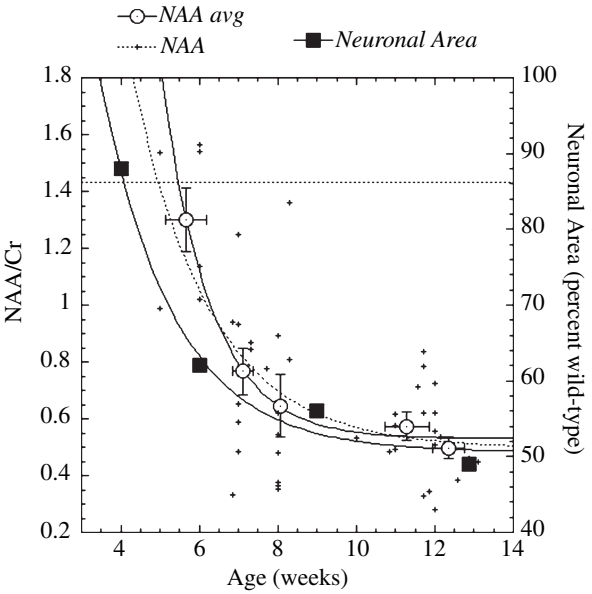

Fig. 5 Comparison of NAA loss and neuronal area as a function of time in the R6/2 mice with 150 CAG repeats. There is an exponential decrease in NAA and, apparently, neuronal area. The crosses are individual data points, the circles are the average NAA values and the squares are the neuronal areas. The fits are to the equation shown in the text, and the dotted line represents the wild-type NAA values which are identical to the pre-symptomatic R6/2 values.

(Jenkins *et al*. 2000). These latter changes parallel those found in the HD model of quinolinic acid lesioned striatum (Tkac *et al*. 2001), and have also been found in extracellular measurements of glutamine in R6/2 mice (Behrens *et al*. 2002). Both we and others showed profound alterations in glucose metabolism in these mice that lead to frank diabetes at late ages (Hurlbert *et al*. 1999; Jenkins *et al*. 2000). They also show increases in neuronal nuclear inclusion bodies (Davies *et al*. 1997) roughly linearly with time (in contrast to the exponential changes in NAA and neuronal area) (Ferrante *et al*. 2000). Since NAA is a marker for both neuronal health and number, the decrease observed in these mice is consistent with the observed decrease in neuronal area. The mice do not show loss of neuronal numbers at 12 weeks-of-age (Jenkins *et al*. 2000). The increased taurine may relate to the decrease in brain volume observed in this and other studies, as taurine has been implicated in playing a role in brain volume regulation (Law 1994) as well as in maintenance of neuronal osmolarity (Burton 1983; Law 1994). Such a role has also been implicated for inositols in the brain. We previously

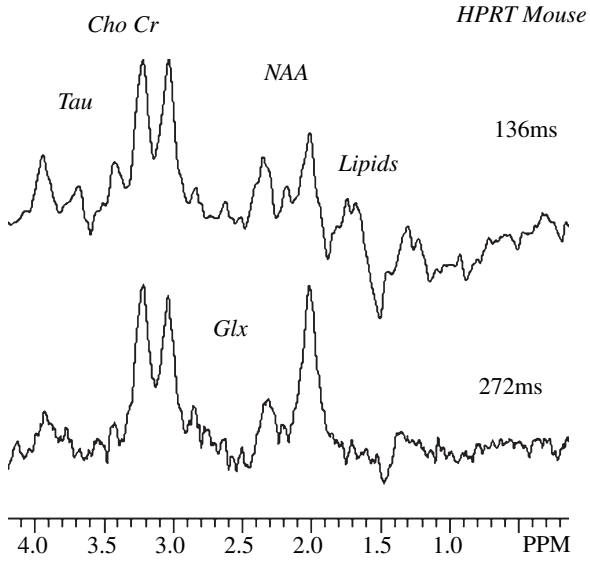

Fig. 6 Representative spectra from HPRT mouse striatum at intermediate and long echo times. Note the large amount of mobile lipids apparent at the 136 ms echo time. These disappear at 272 ms.

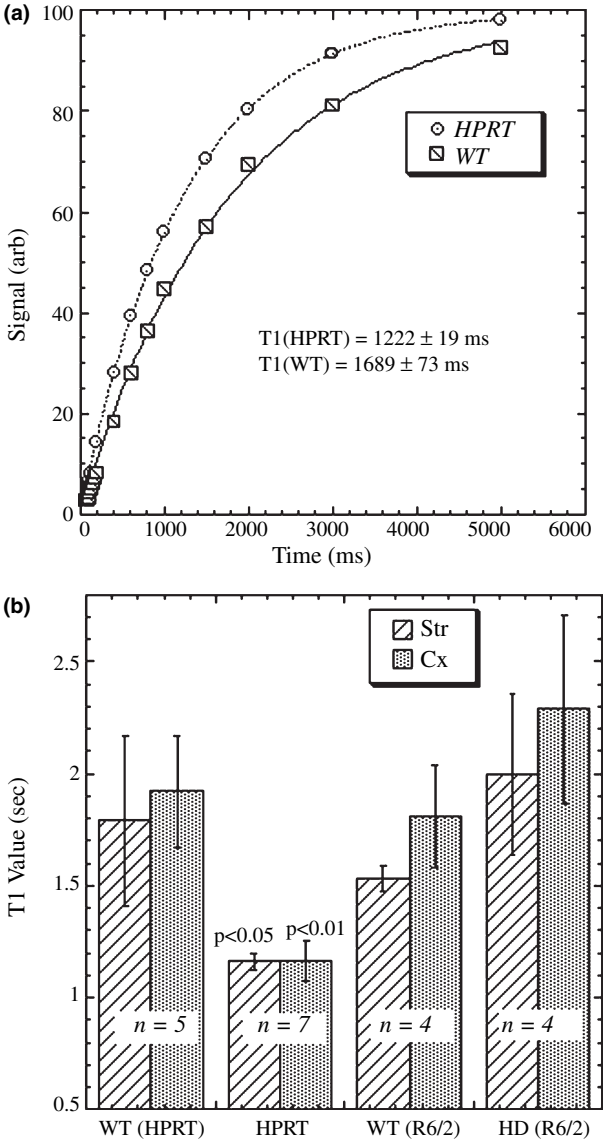

Fig. 7 (a) Plot of signal recovery from a saturation recovery T1 experiment in an HPRT and wild-type mouse showing the shorter T1 in the HPRT striatum. (b) Bar graph of T1 values in wild-type (HPRT), wild-type (R6/2), R6/2 and HPRT mice. The T1 values were significantly shorter in both cortex and striatum in the HPRT mice compared with either the wild-type or R6/2 mice.

observed an increase in scyllo-, but not myo-inostitol in the R6/2 mice using *in vitro* NMR spectroscopy of brain extracts. Taurine and scyllo-inositol resonances at 3.4 ppm overlap in the *in vivo* spectra. However it is likely that most of what we observe is taurine, given the low concentration of scyllo-inositol. The R6/2 mice also show an increase in lactate *in vivo* compared with wild-types. The increase is not as large as that observed in models of HD induced, for example, by quinolinic acid (Tkac *et al*. 2001), but it is similar to that observed in HD patients (Jenkins *et al*. 1993, 1998).

We determined that the onset of NAA loss occurs at about 5 weeks-of-age, coincident with the neuronal area changes. Recent studies of these mice using gene array screening showed that the N-terminal fragment of mutant huntingtin caused down-regulation of striatal signaling genes (Luthi-Carter *et al*. 2002). This latter study of the expression of about 11 000 genes showed that down-regulation of mRNA expression could only be detected starting at about 4 weeks-of-age, close in time to the NAA loss, as well as to the very early behavioral and pathological changes.

In contrast to the R6/2 mice, the N171-82Q mice show a milder phenotype with longer life spans (approximately 135 days vs. 98 days in the R6/2 mice) (Schilling *et al*. 1999). Nonetheless, profound motor abnormalities develop in these mice. As a control we also studied N171-18Q mice with 18 CAG repeats. The latter mice showed a near normal life span, and did not develop overt motor symptoms. In the N171-82Q mice there was a large linear decrease over time in NAA levels in the striatum that paralleled a linear decrease in neuronal area. The cortex was relatively unaffected, similar to the differences found between the cortex and striatum in nuclear inclusions and neuritic aggregates (Schilling *et al*. 1999). Taurine also showed an increase with time in the striatum, similar to that which is seen in the R6/2 mice. Interestingly, in the N171-18Q mice the striatal NAA levels were slightly lower than in wild-type mice. Thus, NAA may prove to be a sensitive marker for subtle signs of pathology. There was no striatal cell loss in the N171-82Q at 120 days-of-age (Schilling *et al*. 1999). How-

Table 3 Summary of *in vivo* MRS data from HPRT and wild-type mice

Mouse	NAA/Cr	Glx/Cr	Cho/Cr	Tau/Cr
HPRT Striatum ($n = 6$)	1.28 ± 0.17*	0.27 ± 0.14	1.10 ± 0.13*	0.13 ± 0.1
WT Striatum ($n = 9$)	1.63 ± 0.19	0.22 ± 0.17	0.92 ± 0.12	0.18 ± 0.09

Data from spectra collected with a TE of 272ms. WT, wild-type. *Significantly different from WT.

ever, similar to the situation found in R6/2 mice, the neurons are shrunken and atrophic (Ferrante *et al*. 2000; Andreassen *et al*. 2001b). This likely explains the large NAA decrease. These mice also demonstrate glucose metabolic abnnormalities. Unlike the R6/2 mice, fewer became frankly diabetic, but after 10 weeks-of-age, glucose intolerance developed with increased fasting blood glucose levels and abnormal glucose tolerance tests, as well as decreased insulin levels (Andreassen *et al*. 2001b).

The YAC mice show a milder phenotype still compared with either the R6/2 or the N171-82Q mice. Two different strains of these mice were originally generated with differing expression levels of the 72 CAG repeat (Hodgson *et al*. 1999). Mice with a higher expression level show a more profound phenotype, similar in many ways to the N171-82Q mice, that is also selective to the striatum and spares the cortex. The strain we studied, the 2511 line, showed a very mild phenotype, whose abnormalities appeared primarily in electrophysiological data. While we did not specifically measure expression levels in this study, our results are consistent with a very mild phenotype. Brain mitochondria isolated from these mice have a decreased capacity for uptake of calcium and more readily undergo the mitochondrial permeability transition compared with wild-type mice or mice with only 18 CAG repeats (Panov *et al*. 2002). Otherwise, these mice have a relatively normal life span and no motor symptoms. Nonetheless, we found a small, but significant decrease in NAA levels in the striatum but not in the cerebral cortex. The mice have spectral abnormalities similar in magnitude to the N171-18Q mice. The N171-18Q mice (18 CAG repeats) have only an N-terminal fragment of the htt protein, whereas the YAC72 mice have the full-length mutant htt protein. This fact accords with the observation that shorter protein fragments of huntingtin are more toxic than the full-length copies (Hackam *et al*. 1998).

The effect of gene context on a 150 repeat CAG expansion was previously examined in the HPRT mice (Ordway *et al*. 1997, 1999). These authors concluded that a number of similar toxic features are conferred by CAG expansion alone, independent of gene context. For instance, intranuclear inclusion bodies seem to be a feature of all the CAG expansions, although this appears to be a feature common to many neurodegenerative disorders (Everett & Wood 2004). The nuclear inclusions in the HPRT mice are widely distributed in the brain, as they are in the R6/2 mice. The HPRT mice we studied are also reported to have handling-induced seizures like those noted in the R6/2 mice (Ordway *et al*. 1997). In spite of these similarities to the R6/2 mice, there are a number of important differences. The HPRT mice live considerably longer than the R6/2 strain, with a median survival of 45 weeks-of-age, and show a late onset of motor symptoms such as impaired activity and rotarod performance (Ordway *et al*. 1997). In addition, these mice gain weight, becoming larger than wild-type mice, compared with the R6/2 mice which lose weight compared with the wild-type. The increase in weight appears to be associated with increases in free brain lipids, as noted by both increased resonance intensity in the upfield region of the spectrum and decreased brain water T1 values. This decrease in brain water T1 is quite large (30%) and opposite in direction to the changes noted in R6/2 mice where T1 values increase. This is apparently not a good model of Lesch–Nyhan syndrome (a congenital deficiency of the HPRT enzyme), and the phenotype in the HPRT mice is consistent with a gain of function associated with the increased CAG repeat in addition to the deficiencies caused by malfunction of the HPRT gene itself (Ordway *et al*. 1997).

While CAG repeat length is clearly one of the most important variables affecting pathology and progression in these different mouse strains, it is by no means the only important variable. In this regard it is important to point out that there are many other differences between these different mouse strains besides just CAG repeat length. One important variable would appear to be the length of the mutant htt protein. Strains with shorter N-terminal fragments, such as the R6/2 mice, have more severe phenotypes than those with full-length mutant proteins, even when adjusted for CAG repeat length. A recent study using gene array technology showed more differences in mRNA expression for the short-length N-terminal genes than those with the full-length genes (Chan *et al*. 2002). This factor may be reflected in our data showing similar NAA loss in the N18 and YAC72 mice we studied. Nonetheless, it is clear that CAG length is still the primary factor in conferring toxicity of mutant htt.

This study emphasises the value of non-invasive MR techniques for longitudinal monitoring of disease progression in transgenic HD mouse models. The decline of NAA seems to be an early and sensitive marker for neuronal dysfunction in these mice. We previously examined the effects of CAG repeat loss in NAA levels in the striatum of HD patients (Jenkins *et al*. 1998). These results indicated that when normalized for age, there was an apparently linear effect of CAG repeat on NAA decline, and that this correlated with

cell loss numbers determined using histopathology (Furtado *et al*. 1996; Penney *et al*. 1997). However, most of the correlation for NAA and histopathology data derives from the higher repeat numbers (CAG > 45). The different rates of NAA loss in the R6/2 and N171-82Q mice support the finding that the rate of progression is CAG repeat length-dependent. One problem in evaluating human populations is that the vast majority of subjects have CAG repeat lengths of less than or equal to 50.

The spectra we collected at 4.7T are not of sufficient quality to separate glutamate from glutamine. We previously showed decreased glutamate and increased glutamine in R6/2 mice using high resolution spectroscopy of brain extracts (Jenkins *et al*. 2000). The advent of even higher field magnets such as 7T and 9.4T will enable *in vivo* separation of glutamate and glutamine, and will thus allow for additional parameters with which to follow the metabolic derangements (Pfeuffer *et al*. 1999). Aside from this observation, however, the increases in taurine and choline are representative of other aspects of the pathology in addition to neuronal dysfunction, possibly involving the nuclear inclusions. The results here confirm that MRS will be useful for following neuroprotective strategies in these mice, as we have shown previously (Ferrante *et al*. 2000; Andreassen *et al*. 2001a,b). However, they also highlight the fact that it is imperative to study multiple time points in the measurement in order to optimize the sensitivity of the MRS exam for following neuroprotective strategies.

Our results also indicate the profound effect of CAG repeat length upon neuronal dysfunction in these mouse models. The abnormalities noted in the N171-18Q and YAC72 mice, however, also indicate the important effects of gene expression levels and transgene type upon the neuronal abnormalities.

Acknowledgements

The authors gratefully acknowledge the generous donation of the HPRT mice from Dr Peter Detloff of the University of Alabama, Birmingham, AL. The work was supported by grant NIH RO1 5R01 NS39258-04.

References

Andreassen O. A., Jenkins B. G., Dedeoglu A., Ferrante K. L., Bogdanov M. B., Kaddurah-Daouk R. and Beal M. F. (2001a) Increases in cortical glutamate concentrations in transgenic amyotrophic lateral sclerosis mice are attenuated by creatine supplementation. *J. Neurochem.* **77**, 383–390.

Andreassen O. A., Dedeoglu A., Ferrante R. J. *et al.* (2001b) Creatine increases survival and delays motor symptoms in a transgenic animal model of Huntington's disease. *Neurobiol. Dis.* **8**, 479–491.

Andrew S. E., Goldberg Y. P., Kremer B. *et al.* (1993) The relationship between trinucleotide (CAG) repeat length and clinical features of Huntington's disease. *Nat. Genet.* **4**, 398–403.

Behrens P. F., Franz P., Woodman B., Lindenberg K. S. and Landwehrmeyer G. B. (2002) Impaired glutamate transport and glutamate-glutamine cycling: downstream effects of the Huntington mutation. *Brain* **125**, 1908–1922.

Burton R. F. (1983) The composition of animal cells: solutes contributing to osmotic pressure and charge balance. *Comp. Biochem. Physiol. [B]* **76**, 663–671.

Chan E. Y., Luthi-Carter R., Strand A. *et al.* (2002) Increased huntingtin protein length reduces the number of polyglutamine-induced gene expression changes in mouse models of Huntington's disease. *Hum. Mol. Genet.* **11**, 1939–1951.

Davies S. W., Turmaine M., Cozens B. A., DiFiglia M., Sharp A. H., Ross C. A., Scherzinger E., Wanker E. E., Mangiarini L. and Bates G. P. (1997) Formation of neuronal intranuclear inclusions underlies the neurological dysfunction in mice transgenic for the HD mutation. *Cell* **90**, 537–548.

Dedeoglu A., Choi J.-K., Cormier K., Kowall N. and Jenkins B. G. (2004) Magnetic resonance spectroscopic analysis of Alzheimer's disease mouse brain that express mutant human APP shows altered neurochemical profile. *Brain Res.* **1012**, 60–65.

van Dellen A., Welch J., Dixon R. M., Cordery P., York D., Styles P., Blakemore C. and Hannan A. J. (2000) N-Acetylaspartate and DARPP-32 levels decrease in the corpus striatum of Huntington's disease mice. *Neuroreport* **11**, 3751–3757.

Dunlop D. S., McHale D. M. and Lajtha A. (1992) Decreased brain N-acetylaspartate in Huntington's disease. *Brain Res.* **580**, 44–48.

Everett C. M. and Wood N. W. (2004) Trinucleotide repeats and neurodegenerative disease. *Brain* **127**, 2385–2405.

Ferrante R. J., Andreassen O. A., Jenkins B. G., Dedeoglu A., Kuemmerle S., Kubilus J. K., Kaddurah-Daouk R., Hersch S. M. and Beal M. F. (2000) Neuroprotective effects of creatine in a transgenic mouse model of Huntington's disease. *J. Neurosci.* **20**, 4389–4397.

Furtado S., Suchowersky O., Rewcastle B., Graham L., Klimek M. L. and Garber A. (1996) Relationship between trinucleotide repeats and neuropathological changes in Huntington's disease. *Ann. Neurol.* **39**, 132–136.

Gauthier L. R., Charrin B. C., Borrell-Pages M. *et al.* (2004) Huntingtin controls neurotrophic support and survival of neurons by enhancing BDNF vesicular transport along microtubules. *Cell* **118**, 127–138.

Hackam A. S., Singaraja R., Wellington C. L., Metzler M., McCutcheon K., Zhang T., Kalchman M. and Hayden M. R. (1998) The influence of huntingtin protein size on nuclear localization and cellular toxicity. *J. Cell Biol.* **141**, 1097–1105.

Hamilton W. C. (1965) Significance tests on the crystallographic R factor. *Acta Crystal.* **18**, 502–510.

Hoang T. Q., Bluml S., Dubowitz D. J., Moats R., Kopyov O., Jacques D. and Ross B. D. (1998) Quantitative proton-decoupled 31P MRS and 1H MRS in the evaluation of Huntington's and Parkinson's diseases. *Neurology* **50**, 1033–1040.

Hodgson J. G., Agopyan N., Gutekunst C. A. *et al.* (1999) A YAC mouse model for Huntington's disease with full-length mutant huntingtin, cytoplasmic toxicity, and selective striatal neurodegeneration. *Neuron* **23**, 181–192.

Huntington's Disease Collaborative Research Group (1993) A novel gene containing a trinucleotide repeat that is expanded and unstable on Huntington's disease chromosomes. *Cell* **72**, 971–983.

Hurlbert M. S., Zhou W., Wasmeier C., Kaddis F. G., Hutton J. C. and Freed C. R. (1999) Mice transgenic for an expanded CAG repeat in the Huntington's disease gene develop diabetes. *Diabetes* **48**, 649–651.

Jenkins B. G., Koroshetz W. J., Beal M. F. and Rosen B. R. (1993) Evidence for impairment of energy metabolism *in vivo* in Huntington's disease using localized 1H NMR spectroscopy. *Neurology* **43**, 2689–2695.

Jenkins B. G., Rosas H. D., Chen Y. C., Makabe T., Myers R., MacDonald M., Rosen B. R., Beal M. F. and Koroshetz W. J. (1998) 1H NMR spectroscopy studies of Huntington's disease: correlations with CAG repeat numbers. *Neurology* **50**, 1357–1365.

Jenkins B. G., Klivenyi P., Kustermann E., Andreassen O. A., Ferrante R. J., Rosen B. R. and Beal M. F. (2000) Nonlinear decrease over time in N-acetyl aspartate levels in the absence of neuronal loss and increases in glutamine and glucose in transgenic Huntington's disease mice. *J. Neurochem.* **74**, 2108–2119.

Law R. O. (1994) Regulation of mammalian brain cell volume. *J. Exp. Zool.* **268**, 90–96.

Lin X., Antalffy B., Kang D., Orr H. T. and Zoghbi H. Y. (2000) Polyglutamine expansion down-regulates specific neuronal genes before pathologic changes in SCA1. *Nat. Neurosci.* **3**, 157–163.

Luthi-Carter R., Strand A., Peters N. L. *et al.* (2000) Decreased expression of striatal signaling genes in a mouse model of Huntington's disease. *Hum. Mol. Genet.* **9**, 1259–1271.

Luthi-Carter R., Hanson S. A., Strand A. D. *et al.* (2002) Dysregulation of gene expression in the R6/2 model of polyglutamine disease: parallel changes in muscle and brain. *Hum. Mol. Genet.* **11**, 1911–1926.

Mangiarini L., Sathasivam K., Seller M. *et al.* (1996) Exon 1 of the HD gene with an expanded CAG repeat is sufficient to cause a progressive neurological phenotype in transgenic mice. *Cell* **87**, 493–506.

Nucifora F. C., Jr, Sasaki M., Peters M. F. *et al.* (2001) Interference by huntingtin and atrophin-1 with cbp-mediated transcription leading to cellular toxicity. *Science* **291**, 2423–2428.

Ordway J. M., Tallaksen-Greene S., Gutekunst C. A. *et al.* (1997) Ectopically expressed CAG repeats cause intranuclear inclusions and a progressive late onset neurological phenotype in the mouse. *Cell* **91**, 753–763.

Ordway J. M., Cearley J. A. and Detloff P. J. (1999) CAG-polyglutamine-repeat mutations: independence from gene context. *Phil. Trans. R. Soc. Lond. B. Biol. Sci.* **354**, 1083–1088.

Panov A. V., Gutekunst C. A., Leavitt B. R., Hayden M. R., Burke J. R., Strittmatter W. J. and Greenamyre J. T. (2002) Early mitochondrial calcium defects in Huntington's disease are a direct effect of polyglutamines. *Nat. Neurosci.* **5**, 731–736.

Penney J. B., Jr, Vonsattel J. P., MacDonald M. E., Gusella J. F. and Myers R. H. (1997) CAG repeat number governs the development rate of pathology in Huntington's disease. *Ann. Neurol.* **41**, 689–692.

Pfeuffer J., Tkac I., Provencher S. W. and Gruetter R. (1999) Toward an *in vivo* neurochemical profile: quantification of 18 metabolites in short-echo-time (1) H NMR spectra of the rat brain. *J. Magn. Reson.* **141**, 104–120.

Sanchez-Pernaute R., Garcia-Segura J. M., del Barrio Alba A., Viano J. and de Yebenes J. G. (1999) Clinical correlation of striatal 1H MRS changes in Huntington's disease. *Neurology* **53**, 806–812.

Schilling G., Becher M. W., Sharp A. H. *et al.* (1999) Intranuclear inclusions and neuritic aggregates in transgenic mice expressing a mutant N-terminal fragment of huntingtin. *Hum. Mol. Genet.* **8**, 397–407.

Snell R. G., MacMillan J. C., Cheadle J. P., Fenton I., Lazarou L. P., Davies P., MacDonald M. E., Gusella J. F., Harper P. S. and Shaw D. J. (1993) Relationship between trinucleotide repeat expansion and phenotypic variation in Huntington's disease. *Nat. Genet.* **4**, 393–397.

Tkac I., Keene C. D., Pfeuffer J., Low W. C. and Gruetter R. (2001) Metabolic changes in quinolinic acid-lesioned rat striatum detected non-invasively by *in vivo* (1)H NMR spectroscopy. *J. Neurosci. Res.* **66**, 891–898.

Wheeler S. L., Khalsa G. J. and Nickoloff J. A. (1999) PCR alone is insufficient for identifying structural modifications to yeast chromosomes. *Biotechniques* **26**, 238–240.